J|A|C|S
ARTICLES
Published on Web 04/12/2003

First Soluble M@C_{60} Derivatives Provide Enhanced Access to Metallofullerenes and Permit in Vivo Evaluation of Gd@C_{60}[$C(COOH)_2$]$_{10}$ as a MRI Contrast Agent

Robert D. Bolskar,*,† Angelo F. Benedetto,‡ Lars O. Husebo,‡ Roger E. Price,§ Edward F. Jackson,§ Sidney Wallace,§ Lon J. Wilson,‡ and J. Michael Alford†

Contribution from TDA Research Inc., 12345 West 52nd Avenue, Wheat Ridge, Colorado 80033, the Department of Chemistry and the Center for Nanoscale Science and Technology, MS-60, Rice University, Houston, Texas 77251-1892, and the MD Anderson Cancer Center, The University of Texas, 1515 Holcombe Boulevard, Houston, Texas 77030-4009

Received January 9, 2003; E-mail: bolskar@tda.com

Abstract: M@C_{60} and related endohedral metallofullerenes comprise a significant portion of the metallofullerene yield in the traditional arc synthesis, but their chemistry and potential applications have been largely overlooked because of their sparse solubility. In this work, procedures are described to solublize Gd@C_{60} species for the first time by forming the derivative, Gd@C_{60}[$C(COOCH_2CH_3)_2$]$_{10}$, and its hydrolyzed water-soluble form, Gd@C_{60}[$C(COOH)_2$]$_{10}$. Imparting water solubility to Gd@C_{60} permits its evaluation as a magnetic resonance imaging (MRI) contrast agent. Relaxometry measurements for Gd@C_{60}[$C(COOH)_2$]$_{10}$ reveal it to possess a relaxivity (4.6 mM^{-1} s^{-1} at 20 MHz and 40 °C) comparable to that of commercially available Gd(III) chelate-based MRI agents. An in vivo MRI biodistribution study in a rodent model reveals Gd@C_{60}[$C(COOH)_2$]$_{10}$ to possess the first non-reticuloendothelial system (RES) localizing behavior for a water-soluble endohedral metallofullerene species, consistent with its lack of intermolecular aggregation in solution as determined by light-scattering measurements. This first derivatization and use of a M@C_{60} species suggests new potential for metallofullerene technologies by reducing reliance on the chromatographic purification procedures normally employed for the far less abundant M@C_{82} and related endohedrals. The recognition that water-soluble fullerene derivatives can be designed to avoid high levels of RES uptake is an important step toward fullerene-based pharmaceutical development.

Introduction

Endohedral fullerenes consist of fullerene cages that encapsulate atoms, clusters, or small molecules.[1,2] The prototypical carbon arc synthesis produces mostly insoluble carbonaceous material (ca. 80%) and soluble empty fullerenes (ca. 15%), while the typical solvent-extractable metallofullerene yield is ca. 1 wt %.[2,3] However, the *total* metallofullerene product can greatly exceed this, particularly when M is a lanthanide element. For example, previous measurements revealed that only 4% of sublimable Gd endohedrals are of the soluble Gd@C_{82} variety, with the balance of the material not soluble in solvents that normally dissolve fullerenes (hydrocarbons, arenes and haloarenes, carbon disulfide, etc.).[4] Because of this insolubility, M@C_{60} species have been largely overlooked, and they remain somewhat enigmatic. Small amounts of M@C_{60} species have been solubilized as electroreduced anions[4] and by extraction with chemically noninnocent amine bases such as aniline and pyridine.[5−7] In contrast, the routine solubility of the M@C_{82} class of metallofullerenes allows handling in a manner similar to that of soluble C_{2n} fullerenes, but their separation still requires labor-intensive and expensive multistep HPLC purification,[2,3] a limitation hampering advancement of metallofullerene-based applications.

Here, we describe a method for utilizing the previously unused, insoluble metallofullerene fractions. The more abundant M@C_{60} fraction of endohedrals (consisting of mostly M@C_{60}, M@C_{70}, and M@C_{74}, and hereafter designated as "M@C_{60}") is separated as a mixture from the soluble empty C_{2n} and soluble

† TDA Research.
‡ Rice University.
§ MD Anderson.

(1) Chai, Y.; Guo, T.; Jin, C.; Haufler, R. E.; Chibante, L. P. F.; Fure, J.; Wang, L.; Alford, J. M.; Smalley, R. E. *J. Phys. Chem.* **1991**, *95*, 7564.
(2) (a) Bethune, D. S.; Johnson, R. D.; Salem, J. R.; de Vries, M. S.; Yannoni, C. S. *Nature* **1993**, *366*, 123. (b) Nagase, S.; Kobayashi, K.; Akasaka, T. *Bull. Chem. Soc. Jpn.* **1996**, *69*, 2131. (c) Liu, S.; Sun, S. *J. Organomet. Chem.* **2000**, *599*, 74. (d) Nagase, S.; Kobayashi, K.; Akasaka, T.; Wakahara, T. In *Fullerenes Chemistry, Physics, and Technology*; Kadish, K. M., Ruoff, R. S., Eds.; John Wiley & Sons: New York, 2000; p 395. (e) Shinohara, H. *Rep. Prog. Phys.* **2000**, *63*, 843.
(3) Shinohara, H.; Yamaguchi, H.; Hayashi, N.; Sato, H.; Ohkohchi, M.; Ando, Y.; Saito, Y. *J. Phys. Chem.* **1993**, *97*, 4259.
(4) Diener, M. D.; Alford, J. M. *Nature* **1998**, *393*, 668.
(5) (a) Kubozono, Y.; Maeda, H.; Takabayashi, Y.; Hiraoka, K.; Nakai, T.; Kashino, S.; Emura, S.; Ukita, S.; Sogabe, T. *J. Am. Chem. Soc.* **1996**, *118*, 6998. (b) Inoue, T.; Kubozono, Y.; Kashino, S.; Takabayashi, Y.; Fujitaka, K.; Hida, M.; Inoue, M.; Kanbara, T.; Emura, S.; Uruga, T. *Chem. Phys. Lett.* **2000**, *316*, 381. (c) Kanbara, T.; Kubozono, Y.; Takabayashi, Y.; Fujiki, S.; Iida, S.; Haruyama, Y.; Kashino, S.; Emura, S.; Akasaka, T. *Phys. Rev. B* **2001**, *64*, 113403.
(6) Ogawa, T.; Sugai, T.; Shinohara, S. *J. Am. Chem. Soc.* **2000**, *122*, 3538.
(7) Solodovnikov, S. P.; Tumanskii, B. L.; Bashilov, V. V.; Lebedkin, S. F.; Skolov, V. I. *Russ. Chem. Bull.* **2001**, *50*, 2242.

10.1021/ja0340984 CCC: $25.00

$M@C_{2n}$ metallofullerenes, and subsequently solubilized through derivatization chemistry. The new derivatives of $Gd@C_{60}$ described below, including $Gd@C_{60}[C(COOCH_2CH_3)_2]_{10}$ and $Gd@C_{60}[C(COOH)_2]_{10}$, are the first highly soluble, air-stable discrete molecules based on the more abundant $M@C_{60}$ fraction of metallofullerenes.

Derivatized fullerenes hold promise for medicinal applications.[8,9] For example, C_{60} derivatives have been shown to inhibit HIV protease,[10] carboxylated C_{60} derivatives are potent antioxidants and act as neuroprotectants in vivo,[11] and endohedral metallofullerenes offer potential in medicine as they present a unique motif for metal ion "superchelation" based on entrapment of metal ions in the fullerene interior space. In this regard, diagnostic and therapeutic nuclear medicine are among the proposed applications.[8,12,13] Gd-containing metallofullerenes are currently being pursued as a new generation of magnetic resonance imaging (MRI) contrast agents[8,14,15] because of their high relaxivities and complete lack of Gd^{3+} ion release under metabolic processes. Toward this goal, using a new water-soluble $Gd@C_{60}[C(COOH)_2]_{10}$ derivative, we demonstrate here the first metallofullerene-based MRI contrast agent having a favorable biodistribution similar to those of existing clinically employed MRI contrast agents. The use of carboxyl functional groups to water solubilize Gd-metallofullerenes has resolved the earlier problem of excess reticuloendothelial system (RES) uptake as seen for polydroxylated fullerene derivatives.

Results and Discussion

$M@C_{60}$ Species and Production of the $Gd@C_{60}$ Fraction Starting Material. $M@C_{60}$ and related metallofullerenes are a class of molecules completely insoluble in the usual fullerene solvents. Their insolubility arises from intermolecular polymerization caused, at least in part, by their open-shell electronic configuration and small HOMO−LUMO gaps.[4] Largely because of the $M@C_{60}$-class insolubility, much of the previous work with metallofullerenes has instead focused on the soluble $M@C_{82}$ class.[2] Although this class also has open-shell electronic configurations, the intermolecular association of certain $M@C_{82}$ isomers is apparently much weaker because of significant electron density localization of the unpaired electron inside the fullerene cage.[16] The reported processes for isolating these soluble $M@C_{82}$ species from the products of arc synthesis are labor-intensive and expensive, relying on multistep HPLC purification using costly specialty columns.[2,3] In addition, some of the $M@C_{82}$ species are air sensitive. Higher yields of soluble $Sc_3N@C_{80}$ and related endohedrals have been reported,[17] but their purification still relies on costly and time-consuming HPLC separations of minor components of the arc process. For these reasons, the relatively low availability of metallofullerenes has hampered the advancement of metallofullerene-based applications.

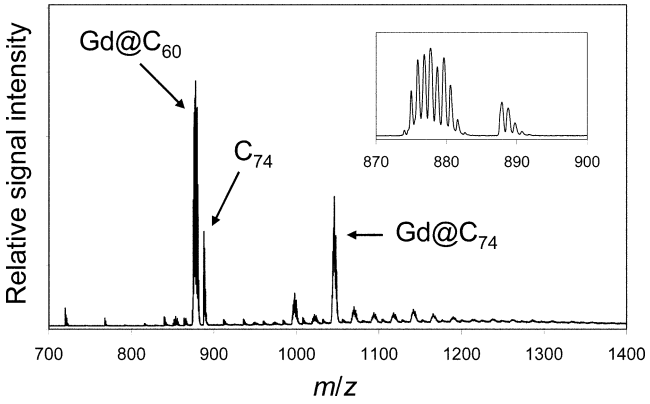

Figure 1. Positive-ion LD-TOF mass spectrum of the "$Gd@C_{60}$ class" of fullerenes. (Inset) Expansion of the 870−900 mass region, showing the isotope patterns for $Gd@C_{60}$ and the empty fullerene, C_{74}.

We have pursued the chemistry of the more abundant $M@C_{60}$ class as a step toward generating larger quantities of metallofullerene-based materials. Here, the $Gd@C_{60}$ class of endohedral metallofullerenes was developed first because of our interest in their potential as MRI contrast agents. Gd-containing fullerenes were generated by the standard DC arc discharge of Gd_2O_3-impregnated graphite rods, using cathode deposit "backburning" to maximize the total yield of fullerenes per arc run. Sublimation at 750 °C and 1 mTorr separated the fullerenes (including both soluble and insoluble empty fullerenes and $Gd@C_{2n}$ endohedrals) from the nonfullerene carbon soot.[4,18] Exploiting the insolubility of the $M@C_{60}$ class, the *soluble* C_{2n} and $Gd@C_{2n}$ fullerenes were removed from the sublimate by repeated *o*-dichlorobenzene washings using a Soxhlet extractor operating at 40 Torr and 100 °C, until the washings were colorless. The collection of the sublimate and the Soxhlet extraction were performed anaerobically inside an argon-filled glovebox due to the air sensitivity of some endohedral fullerene materials.[2,19]

Reductive and oxidative treatments of mixed endohedral fullerene materials can be used to separate fractions of fullerenes having similar redox properties from other components with differing redox properties.[4,20] Here, a chemically oxidative treatment was used to enrich the $Gd@C_{60}$ content of the insoluble material by solubilizing and removing several percent of oxidizable $Gd@C_{2n}$ ($2n \geq 72$) and C_{74}. The remaining insoluble "$Gd@C_{60}$ fraction" of metallofullerenes, the mass spectrum of which is shown in Figure 1, is composed primarily of $Gd@C_{60}$ and $Gd@C_{74}$, with smaller amounts of $Gd@C_{70}$, empty C_{74}, and other minor $Gd@C_{2n}$ species with $2n > 70$. Only traces of C_{60}, C_{70}, etc. remain in this material. Over 500

(8) Wilson, L. J. *Interface* **1999**, *8* (4, Winter), 24.
(9) Wilson, S. R. In *Fullerenes Chemistry, Physics, and Technology*; Kadish, K. M., Ruoff, R. S., Eds.; John Wiley & Sons: New York, 2000; 437.
(10) Friedman, S. H.; DeCamp, D. L.; Sijbesma, R. P.; Srdanov, G.; Wudl, F.; Kenyon, G. L. *J. Am. Chem. Soc.* **1993**, *115*, 6506.
(11) Dugan, L. L.; Turetsky, D. M.; Du, C.; Lobner, D.; Wheeler, M.; Almli, C. R.; Shen, C.; Luh, T.; Choi, D.; Lin, T. *Proc. Natl. Acad. Sci. U.S.A.* **1997**, *94*, 9434.
(12) (a) Cagle, D. W.; Thrash, T. P.; Alford, M.; Chibante, L. P. F.; Ehrhardt, G. J.; Wilson, L. J. *J. Am. Chem. Soc.* **1996**, *118*, 8043. (b) Wilson, L. J.; Cagle, D. W.; Thrash, T. P.; Kennel, S. J.; Mirzadeh, S.; Alford, J. M.; Ehrhardt, G. J. *Coord. Chem. Rev.* **1999**, *190*−*192*, 199. (c) Thrash, T. P.; Cagle, D. W.; Alford, J. M.; Wright, K.; Ehrhardt, G. J.; Mirzadeh, S.; Wilson, L. J. *Chem. Phys. Lett.* **1999**, *308*, 329.
(13) Cagle, D. W.; Kennel, S. J.; Mirzadeh, S.; Alford, J. M.; Wilson, L. J. *Proc. Natl. Acad. Sci. U.S.A.* **1999**, *96*, 5182.
(14) Zhang, S.; Sun, D.; Li, X.; Pei, F.; Liu, S. *Fullerene Sci. Technol.* **1997**, *5*, 1635.
(15) Mikawa, M.; Kato, H.; Okumura, M.; Narazaki, M.; Kanazawa, Y.; Miwa, N.; Shinohara, H. *Bioconjugate Chem.* **2001**, *12*, 510.
(16) Kessler, B.; Bringer, A.; Cramm, S.; Schlebusch, C.; Eberhardt, W.; Suzuki, S.; Achiba, Y.; Esch, F.; Barnaba, M.; Cocco, D. *Phys. Rev. Lett.* **1997**, *79*, 2289.
(17) Stevenson, S.; Rice, G.; Glass, T.; Harich, K.; Cromer, F.; Jordan, M. R.; Craft, J.; Hadju, E.; Bible, R.; Olmstead, M. M.; Maitra, K.; Fisher, A. J.; Balch, A. L.; Dorn, H. C. *Nature* **1999**, *401*, 55.
(18) Diener, M. D.; Smith, C. A.; Veirs, K. D. *Chem. Mater.* **1997**, *9*, 1773.
(19) Hettich, R.; Lahamer, A.; Zhou, L.; Compton, R. *Int. J. Mass. Spectrom.* **1999**, *182*/*183*, 335.
(20) Bolskar, R. D.; Alford, J. M. *Chem. Commun.* **2003**, in press.

mg of the Gd@C_{60} fraction is readily obtained from ca. 2.5 g of starting sublimate, using this nonchromatographic process. This is a considerably larger amount of material than can be currently obtained by chromatographic separation of only the soluble metallofullerenes, for example Gd@C_{82} or the various soluble $M_3N@C_{2n}$ species such as $Sc_3N@C_{80}$.[2,17] While Gd@C_{60} has yet to be isolated as a pure material, it is the dominant component of this class or fraction of fullerene molecules having very similar properties (see Figure 1).

Gd@C_{60} Derivatization: Sythesis of Gd@C_{60}[C(COOCH$_2$CH$_3$)$_2$]$_{10}$ and Gd@C_{60}[C(COOH)$_2$]$_{10}$. Exohedral derivatization chemistry of metallofullerenes has developed in a manner analogous to that of the soluble C_{2n} fullerenes, but more slowly, due to the scarce amount of available metallofullerene starting material. Akasaka and co-workers reported the first derivatizations of La@C_{82}, Gd@C_{82}, $La_2@C_{80}$, and $Sc_2@C_{84}$ with disiliranes and digermanes.[21] Suzuki and co-workers then reported the reaction of La@C_{82} with substituted diazomethanes to form methanofullerene derivatives.[22] Gu and co-workers reported generation of methanofullerene derivatives of Tb@C_{82} by Cu(I)-catalyzed addition of α-diazocarbonyl compounds.[23] Additionally, several different groups have reported polyhydroxylation of the metallofullerene cages Ho@C_{82}, $Ho_2@C_{82}$, Pr@C_{82}, and Gd@C_{82}.[8,13−15,24] However, these reported derivatizations began with metallofullerenes already soluble in the reaction medium, which in most cases was toluene or a similar "standard" fullerene solvent. In contrast, the new process described below is highly effective toward derivatizing insoluble fullerenes, and it is this exohedral chemical modification which now allows the endohedral fullerenes that previously went unused as waste (including M@C_{60}) to now be utilized.

The cycloaddition reaction widely used to add functionalities across carbon−carbon double bonds of fullerenes is the base-induced Michael addition of malonates first reported for C_{60} by Bingel[25] and later expanded upon by Hirsch and co-workers.[26] These reaction conditions (hydrocarbon solvents such as toluene and sodium hydride or 1,8-diazabicyclo[5.4.0]undec-7-ene (DBU) as the base) are not optimal with metallofullerenes, however. DBU use is not preferred with metallofullerenes because, like basic nitrogen solvents (pyridine, aniline, dimethylformamide, etc.),[5−7] it adds readily to fullerene surfaces,[27] a problem only exacerbated by the metallofullerenes' electronegativity. For the Gd@C_{60}-fraction metallofullerenes, we have developed reaction conditions that derivatize and solubilize the insoluble polymer material without requiring their prior dissolution. Using tetrahydrofuran (THF) as solvent at room temperature with a ca. 15-fold excess of diethyl bromomalonate and alkali metal hydride (NaH or KH), the Gd@C_{60}-fraction material is rapidly derivatized with multiple malonate ester groups, which readily solubilize this otherwise intractable material by breaking up the polymer into individually soluble molecules. Hundreds of milligrams of a dark-brown, highly organic-soluble and air-stable derivative can be obtained in only minutes without heating.

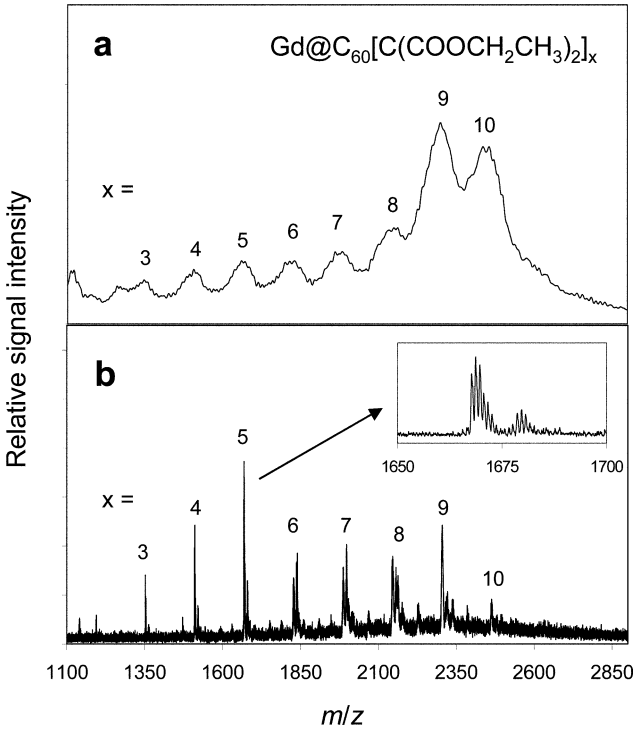

Figure 2. Positive-ion MALDI-TOF mass spectra of the Gd@C_{60}[C(COOCH$_2$CH$_3$)$_2$]$_{10}$ derivative product (S_8 matrix): (a) low-resolution mass spectrum; (b) high-resolution mass spectrum; the inset expands the 1650−1700 mass region.

Mass spectral analysis of this product (Figure 2) reveals it to be chiefly composed of Gd@C_{60}[C(COOCH$_2$CH$_3$)$_2$]$_x$,with the parent ion peak at $x = 10$. Two laser-desorption mass spectra taken under different conditions (see Experimental Section) of this product are shown, Figure 2a with low-resolution conditions and Figure 2b with higher-resolution conditions. Exohedral fullerene derivatives are well-known to fragment in the gas phase under laser desorption and other sampling conditions, generating mass spectral peaks for derivatives having fewer adduct groups per fullerene sphere than are present for the parent compound. Figure 2a shows, despite low resolution, a preponderance of $x = 9$ and 10 for the parent ion peaks, and while Figure 2b does show $x = 10$ for the parent ion peak, it also shows a greater intensity for the lower-mass adduct peaks. Also visible in Figure 2b is the Gd isotope pattern for the derivatives $x = 5$ and lower (see inset) that provides unambiguous evidence for the derivatization of the Gd@C_{60} molecule. The Gd isotope pattern is not readily discernible for the higher-mass adduct peaks, most likely because of the high degree of fragmentation operating with the parent ion and higher adducts. Very minor peaks for other derivatized fullerene cages (e.g., Gd@C_{70}, Gd@C_{74}, etc.; see Figure 1) are also present. The differences between the two spectra in Figure 2 underscore the difficulty in analyzing fullerene derivatives by mass spectroscopy, but the data serves

(21) (a) Akasaka, T.; Kato, T.; Kobayashi, K.; Nagase, S.; Yamamoto, K.; Funasaka, H.; Takahashi, T. *Nature* **1995**, *374*, 600. (b) Akasaka, T.; Nagase, S.; Kobayashi, K.; Suzuki, T.; Kato, T.; Kikuchi, K.; Achiba, Y.; Yamamoto, K.; Funasaka, H.; Takahashi, T. *Angew. Chem., Intl. Ed. Engl.* **1995**, *34*, 2139. (c) Akasaka, T.; Nagase, S.; Kobayashi, K.; Suzuki, T.; Kato, T.; Yamamoto, K.; Funasaka, H.; Takahashi, T. *Chem. Commun.* **1995**, 1343.
(22) Suzuki, T.; Maruyama, Y.; Kato, T.; Akasaka, T.; Kobayashi, K.; Nagase, S.; Yamamoto, K.; Funasaka, H.; Takahashi, T. *J. Am. Chem. Soc.* **1995**, *117*, 9606.
(23) Feng, L.; Zhang, X.; Yu, Z.; Wang, J.; Gu, Z. *Chem. Mater.* **2002**, *14*, 4021
(24) Sun, D.; Huang, H.; Yang, S.; Liu, Z.; Liu, S. *Chem. Mater.* **1999**, *11*, 374.
(25) Bingel, C. *Chem. Ber.* **1993**, *126*, 1957.
(26) Hirsch, A.; Lamparth, I.; Karfunkel, H. R. *Angew. Chem., Int. Ed.* **1994**, *33*, 437.
(27) Skiebe, A.; Hirsch, A.; Klos, H.; Gotschy, B. *Chem. Phys. Lett.* **1994**, *220*, 138.

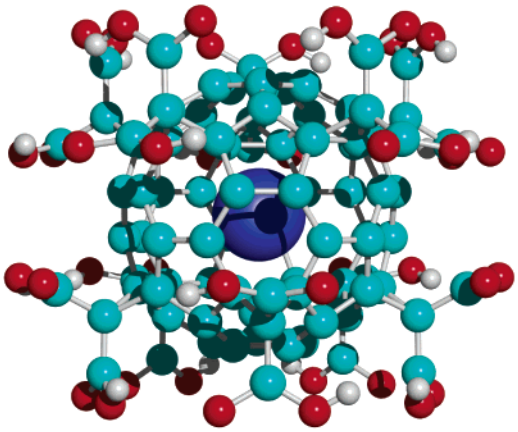

Figure 3. Ball-and-stick depiction of $Gd@C_{60}[C(COOH)_2]_{10}$, illustrating a possible arrangement of 10 $C(COOH)_2$ addends on a single C_{60} cage (light blue, C; red, O; white, H; dark blue, Gd).

to establish the identity of the $Gd@C_{60}[C(COOCH_2CH_3)_2]_{10}$ derivative material.

This ester derivative was readily converted into the water-soluble $Gd@C_{60}[C(COOH)_2]_{10}$ carboxylate acid using the method reported by Hirsch for the conversion of $C_{2n}[C(COOCH_2CH_3)_2]_x$ to the corresponding $C_{2n}[C(COOH)_2]_x$ species.[28] Figure 3 illustrates a likely structural isomer, consistent with the addition pattern proposed for the deca-addition of 1,8-naphthyne to C_{60}.[29]

The first derivatization of $Gd@C_{60}$ reported here is significant for several reasons. It provides a solution to the long-standing problem of how to exploit the polymerized $M@C_{60}$ species that, while more abundant than soluble $M@C_{82}$ metallofullerenes, previously went unused. Using more polar solvents such as tetrahydrofuran (instead of nonpolar hydrocarbons such as toluene) allows the incipient malonate carbanion to derivatize the solid $Gd@C_{60}$ surface in an apparently heterogeneous solid-/solution-phase reaction. The reaction proceeds very rapidly to the deca-addition stage without heating (unlike the traditional Bingel and Hirsch conditions) with the exohedral derivatization breaking up the intermolecular polymerization of $Gd@C_{60}$. Finally, starting from the $Gd@C_{60}$-containing arc product, the process is easily scalable to produce hundreds of milligrams of the water-soluble, air-stable $Gd@C_{60}[C(COOH)_2]_{10}$ product over several days.

Magnetic Relaxivity Measurements. Measuring the r_1 "relaxivity′ of a water-soluble paramagnetic compound is a quantitative way to compare its efficacy in relaxing solvent water protons (shortening T_1 or the longitudinal relaxation time) to that of other paramagnetic ions and their complexes.[30,31] Several different groups have identified water-solubilized polyhydroxyl Gd metallofullerene compounds as potential MRI contrast agents, with each reporting different r_1 values. Zhang et al. measured $r_1 = 47\ mM^{-1}\ s^{-1}$ (at 9.4 T) for a mixed sample of empty fullerene and Gd metallofullerene polyhydroxyl compounds,[14] while Wilson et al. reported $r_1 = 20\ mM^{-1}\ s^{-1}$ for $Gd@C_{82}(OH)_x$ (at 0.47 T and 40 °C).[8] More recently, Shinohara and co-workers reported $Gd@C_{82}(OH)_x$ ($x \approx 40$) with an r_1 value of $67\ mM^{-1}\ s^{-1}$ (at 0.47 T and 25 °C) and $r_1 = 81\ mM^{-1}\ s^{-1}$ (at 1.0 T and 25 °C).[15] These r_1 values are all higher than the relaxivities of clinically used Gd(III) chelates and demonstrate that Gd metallofullerene compounds can serve as potent T_1 relaxation agents for water protons.[32]

In this work, the measured r_1 relaxivity in water for $Gd@C_{60}[C(COOH)_2]_{10}$ is $4.6\ mM^{-1}\ s^{-1}$ (at 20 MHz, 40 °C, and based on Gd content by ICP analysis). This is comparable to the best [Gd^{III}(chelate)] MRI contrast agents in the marketplace today such as ProHance ([Gd(HP-DO3A)(H_2O)]; $r_1 = 3.6\ mM^{-1}\ s^{-1}$) and Magnevist ($[Gd(DTPA)(H_2O)]^{2-}$; $r_1 = 4.3\ mM^{-1}\ s^{-1}$) under similar conditions.[30] For comparison, $La@C_{60}[C(COOH)_2]_x$ was prepared in a manner analogous to that for $Gd@C_{60}[C(COOH)_2]_{10}$. This La-containing metallofullerene should be similar in electronic structure to its Gd analogue, as both contain trivalent endohedral lanthanide metals (resulting in one unpaired electron on the fullerene cage); however, with its d^0 configuration, La^{3+} has no metal-centered unpaired f electrons. The r_1 relaxivity of $La@C_{60}[C(COOH)_2]_x$ in water was determined to be less than $1\ mM^{-1}\ s^{-1}$ (ca. $0.3\ mM^{-1}\ s^{-1}$ at 20 MHz and 40 °C with $x \approx 10$).

These results raise some important points and generate questions about the nature of metallofullerene-induced relaxivity in water. While the magnitude of the relaxivity for $Gd@C_{60}[C(COOH)_2]_{10}$ is nearly the same as for the [Gd^{III}(chelate)] compounds, the relaxation mechanisms must differ, since water molecules have no direct access to a Gd^{3+} ion inside the fullerene carbon cage. Most plausible is an outer-sphere relaxation mechanism with water molecules hydrogen-bonded to the water-solubilizing groups on the fullerene surface, with the unpaired f electrons of the encaged Gd^{3+} ion magnetically coupled to the unpaired electron in the fullerene-centered molecular orbital, which itself transfers some spin density to the substituents. This explanation is consistent with the large drop-off in relaxivity seen in going from the carboxylated $Gd@C_{60}$ compound (seven f electrons) to the $La@C_{60}$ analogue (zero f electrons).

Another issue raised by the relaxivity results for $Gd@C_{60}[C(COOH)_2]_{10}$ is why the relaxivities of $Gd@C_{82}(OH)_x$ compounds are up to an order of magnitude higher. Also unexplained is the significant variation in the r_1 relaxivity values reported for the various $Gd@C_{82}(OH)_x$ preparations. A contributing factor to the former may be the closer proximity of proton-water exchange to the paramagnetic fullerene surface for the polyhydroxyl derivatives. A possible explanation for the latter is that different syntheses of the polyhydroxyl fullerene compounds give somewhat different materials both in number and disposition of the hydroxyl groups. Both of these issues are challenging questions to unravel, since definitive spectroscopic and structural characterization of polyhydroxyl fullerene compounds is difficult to achieve. While the elevated relaxivities of the polyhydroxyl materials remain incompletely explained by the above considerations, a likely explanation does emerge if intermolecular aggregation of water-soluble fullerene compounds is considered.

(28) (a) Lamparth, I.; Hirsch, A. *Chem. Commun.* **1994**, 1727. (b) Lamparth, I.; Schick, G.; Hirsch, A. *Liebigs Ann./Recl.* **1997**, 253.
(29) Hoke, S. H., II; Molstad, J.; Yang, S.-S.; Carlson, D.; Kahr, B. *J. Org. Chem.* **1994**, *59*, 3230.
(30) (a) Lauffer, R. B. *Chem. Rev.* **1987**, *87*, 901. (b) Caravan, P.; Ellison, J. J.; McMurry, T. J.; Lauffer, R. B. *Chem. Rev.* **1999**, *99*, 2293.
(31) Tóth, E.; Helm, L.; Merbach, A. In *The Chemistry of Contrast Agents in Medical Magnetic Resonance Imaging*; Merbach, A., Tóth, E., Eds.; John Wiley & Sons: Chichester, 2001; pp 45−120.

(32) As relaxivity measurements are dependent on temperature and magnetic field, it is most meaningful to compare r_1 values obtained under the same conditions.

Assessing Intermolecular Aggregation. Intermolecularly aggregated MRI contrast agents are known to exhibit increased rotational correlation times, which results in enhanced relaxivities relative to nonaggregated agents.[31,33] Thus, the propensity of water-soluble fullerene derivatives toward intermolecular aggregation or spontaneous clustering in aqueous solution would have consequences for interpreting their measured relaxivities. Indeed, previous independent laser-light scattering, small-angle neutron scattering, and small-angle X-ray scattering measurements on several water-soluble fullerene derivatives provide complimentary experimental evidence for aggregation. Guldi and co-workers have found evidence of aggregation for water-soluble C_{60} derivatives, including $C_{60}(OH)_{18}$ and C_{60}-$[C(COOH)_2]$.[34] Pulse radiolysis and triplet lifetime measurements on the C_{60} monoadduct, $C_{60}[C(COOH)_2]$, suggested aggregation in aqueous solution.[34a,c] Pulse radiolysis and optical absorption spectroscopy with $C_{60}(C_4H_{10}N^+)$ also revealed aggregation for this monoadduct.[34b,c] Guldi concluded that covalent attachment of only one addend to the C_{60} surface was insufficient to prevent hydrophobic attraction and aggregation of these derivatives. Bensasson et al. reported that lower singlet oxygen quantum yields for $C_{60}[C(COOH)_2]_n$ derivatives (with $n = 2-6$) in aqueous solution as compared to those for the corresponding ethyl esters in toluene was indicative of clustering of the acids in water.[35]

Furthermore, dynamic light-scattering measurements on the polyhydroxyl C_{60} compound $C_{60}(OH)_{18}$ showed evidence for aggregates at high solute concentrations (up to 39 mM).[34d] A small-angle X-ray scattering study by Chiang and co-workers measured $C_{60}(OH)_{18}$ aggregates in aqueous solution of 20 Å R_g (R_g = radius of gyration) at 0.7 mM, with the aggregates doubling in size to 40 Å R_g at 50 mM.[36] They also found water-soluble $C_{60}[(CH_2)_4SO_3Na]_6$ to have 19 Å R_g across the range of concentrations from 0.4 to 26 mM in aqueous solution.[36] Dynamic light-scattering measurements on a highly water-soluble dendro-C_{60} monoadduct derivative (having a second-generation bis(polyamide) malonate dendrimer with 18 carboxylate groups) by Brettreich and Hirsch revealed clusters of at least two different size ranges. Clusters with average hydrodynamic radii of ca. 10 and 38 nm were seen at pH = 8, with a decrease in size to 5 nm for the smaller clusters at pH = 11.[37] Chu, Sawamura, Nakamura, and co-workers recently reported that water-soluble $Ph_5C_{60}K$ forms vesicles having a hydrodynamic radius of 17 nm as detected by laser-light scattering.[38] These different examples reveal that intermolecular aggregation of water-soluble fullerene derivatives occurs with a range of different derivative groups having a variety of dispositions on fullerene cages.

Several aggregation mechanisms may contribute to the clustering of these water-soluble fullerene derivatives, including both intermolecular hydrogen bonding and hydrophobic fullerene−fullerene attraction with the degree of aggregation varying with concentration. There may be a minimum level of derivatization needed for sufficient solubility and minimization of hydrophobic interactions, the extent of which is dependent on the fullerene cage as well as the type of derivative group.

Because of the above considerations, we have performed a qualitative assessment of aggregation of water-solubilized Gd@C_{60} compounds by dynamic light scattering (DLS). DLS measurements comparing polyhydroxylated fullerene compounds such as Gd@$C_{60}(OH)_x$ and Gd@$C_{60}[C(COOH)_2]_{10}$ under the same conditions revealed that the polyhydroxylated fullerenes form aggregates in excess of 100 nm in diameter, while Gd@$C_{60}[C(COOH)_2]_{10}$ displayed no aggregation down to the instrumental detection limit (~10 nm). This order-of-magnitude difference in aggregation propensity correlates with the elevated r_1 values seen for the polyhydroxyl compounds in comparison to that for Gd@$C_{60}[C(COOH)_2]_{10}$. Large clusters of slowly tumbling polyhydroxyl fullerenes will have higher relative relaxivities than comparable molecules that are not intermolecularly aggregated. The decamethano Gd@C_{60} compound (with its 20 carboxyl groups) lends itself to less intermolecular aggregation than the polyhydroxylated fullerenes because of its highly charged surface. Also, the steric disposition of the 10 derivative groups (Figure 3) protects the underivatized fullerene surface(s) of Gd@$C_{60}[C(COOH)_2]_{10}$ from hydrophobic-induced aggregation. Thus, the structure and identity of the derivative groups on the Gd@$C_{60}[C(COOH)_2]_{10}$ inhibits intermolecular aggregation that dominates the solution structure of polyhydroxyl fullerene derivatives. Comparative in vivo biodistribution studies of Gd@$C_{60}[C(COOH)_2]_{10}$ and M@$C_{82}(OH)_x$ species also support this aggregation hypothesis, as discussed below.

In Vivo MRI Measurements and Biodistribution Data for Gd@$C_{60}[C(COOH)_2]_{10}$. To study the biodistribution of Gd@C_{60}-$[C(COOH)_2]_{10}$ in vivo, an MR imaging experiment with a rodent model was performed at an approximate dosage of 35 mg/kg, which was well tolerated by the animal. The MR imaging experiment (see Experimental Section) revealed that Gd@C_{60}-$[C(COOH)_2]_{10}$ behaved much like commercially available Gd chelate-based MRI contrast agents (e.g., Prohance and Magnevist) in this animal model.[39] Typical biodistribution results are shown in Figures 4 and 5. The Gd@$C_{60}[C(COOH)_2]_{10}$ agent moved rapidly to the kidneys, with only minimal uptake into the liver as illustrated graphically in Figure 4, which compares the relative MRI enhancement proffered by the metallofullerene derivative in the kidney vs that in the liver in the minutes after injection. Figure 5 shows examples of the MR images obtained, comparing the MRI intensity of one kidney before contrast agent injection and again 16 min after injection. The lighter color of the kidney in the latter image results from the proton relaxation induced by the paramagnetic Gd@$C_{60}[C(COOH)_2]_{10}$ contrast agent. The agent began undergoing excretion via the bladder within 1 h of injection. This biodistribution behavior is in striking contrast to that seen previously with polyhydroxylated fullerene derivatives.

(33) Fatin-Rouge, N.; Toth, E.; Perret, D.; Backer, R. H.; Merbach, A. E.; Bunzli, J.-C. G. *J. Am. Chem. Soc.* **2000**, *122*, 10810.
(34) (a) Guldi, D. M.; Hungerbühler, H.; Asmus, K.-D. *J. Phys. Chem.* **1995**, *99*, 13487. (b) Guldi, D. M.; Hungerbühler, H.; Asmus, K.-D. *J. Phys. Chem. A* **1997**, *101*, 1783. (c) Guldi, D. M. *J. Phys. Chem. A* **1997**, *101*, 3895. (d) Mohan, H.; Palit, D. K.; Mittal, J. P.; Chiang, L. Y.; Asmus, K.-D.; Guldi, D. M. J. *Chem. Soc., Faraday Trans.* **1998**, *94*, 359.
(35) Bensasson, R. V.; Berberan-Santos, M. N.; Brettreich, M.; Frederiksen, J.; Göttinger, H.; Hirsch, A.; Land, E. J.; Leach, S.; McGarvey, D. J.; Schönberger, H.; Schröder, C. *Phys. Chem. Chem. Phys.* **2001**, *3*, 4679.
(36) (a) Jeng, U.-S.; Lin, T.-L.; Chang, T. S.; Lee, H.-Y.; Hsu, C.-H.; Hsieh, Y.-W.; Canteenwala, T.; Chiang, L. Y. *Prog. Colloid Polym. Sci.* **2001**, *118*, 232. (b) Jeng, U.-S.; Lin, T.-L.; Tsao, C.-S.; Lee, C.-H.; Canteenwala, T.; Wang, L. Y.; Chiang, L. Y.; Han, C. C. *J. Phys. Chem. B* **1999**, *103*, 1059.
(37) Brettreich, M.; Hirsch, A. *Tetrahedron Lett.* **1998**, *39*, 2731.
(38) Zhou, S.; Burger, C.; Chu, B.; Sawamura, M.; Nagahama, N.; Toganoh, M.; Hackler, U. E.; Isobe, H.; Nakamura, E. *Science* **2001**, *291*, 1944.
(39) Wedeking, P.; Eaton, S.; Covell, D. G.; Nair, S.; Tweedle, M. F.; Eckelman, W. C. *Magn. Res. Imag.* **1990**, *8*, 567.

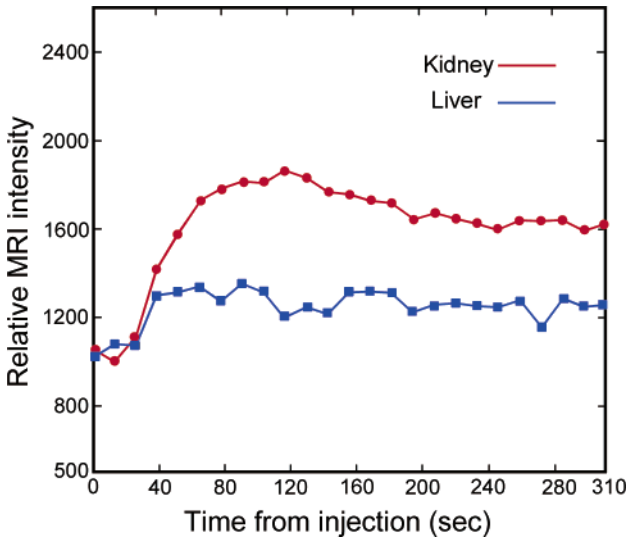

Figure 4. Representative in vivo MRI intensity-derived biodistribution data showing the Gd@C_{60}[C(COOH)$_2$]$_{10}$ signal enhancement within the first 5 min of administration, revealing rapid renal uptake with a minimum of liver uptake (red circles, kidney; blue squares, liver).

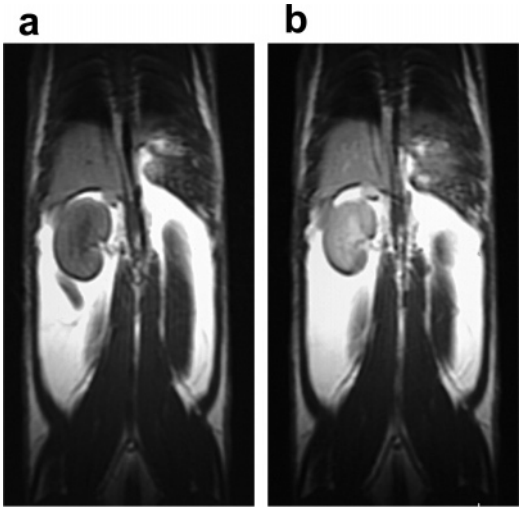

Figure 5. Representative in vivo rodent MR images focusing on a cross section containing a portion of one kidney. (a) Baseline image without contrast agent; (b) image of the same cross section 16 min after administration of Gd@C_{60}[C(COOH)$_2$]$_{10}$ with increased signal intensity in the kidney.

Several complimentary studies on the biodistribution of the polyhydroxylated compounds $^{166}Ho_n@C_{82}(OH)_x$ ($n = 1, 2$; $x \approx 16$), Gd@$C_{82}(OH)_x$ ($x \approx 40$) and ^{99m}Tc-labeled $C_{60}(OH)_x$ have recently revealed high uptake levels of these compounds by the reticuloendothelial system (RES). The radiotracer study conducted by Cagle et al. with $^{166}Ho_n@C_{82}(OH)_x$ ($n = 1, 2$; $x \approx 16$) showed significant RES uptake in mice, including concentration in liver and bone.[13] The MR imaging and biodistribution study performed by Shinohara and co-workers with Gd@$C_{82}(OH)_x$ ($x \approx 40$) reported similar results.[15] Qingnuan et al. have recently published a radiotracer study with the (nonendohedral) polyhydroxyl C_{60} derivative ^{99m}Tc−$C_{60}(OH)_x$.[40] The biodistribution results in mice and rabbits also showed significant uptake of the polyhydroxyl fullerene by the kidneys, bone, spleen, and liver. The common feature in all of these studies is the polyhydroxyl derivatization of the fullerene cage, while the differences among these compounds (different cage sizes, different endohedral metals or lack thereof, different electronic structures, etc.) apparently do not significantly affect the biodistribution. It also appears that differing degrees of hydroxylation do not produce a major impact on the observed biodistributions.

The RES uptake of polyhydroxyl fullerene compounds has important implications for the development of pharmaceuticals based on water-soluble fullerenes. Shinohara and co-workers have noted that polyhydroxyl fullerene compounds induce spontaneous aggregation of erythrocytes when in contact with blood and that addition of mannosyl groups to a polyhydroxyl C_{60} surface diminishes this effect.[41] It is not yet clear if in vivo RES uptake stems from intermolecular aggregation causing larger particles to be targeted by the RES or if the RES uptake results from polyhydroxyl fullerene-induced aggregation of erythrocytes (or other blood components/proteins), which are then targeted by the RES. A combination of the two actions seems plausible, but one must note that the intermolecular clustering as measured by light-scattering techniques and as inferred by relaxivity measurements does not require the presence of blood or blood components to be manifested. For fullerene-based pharmaceuticals to be successful, sufficient water solubility without significant RES uptake is required, and the new Gd@C_{60}[C(COOH)$_2$]$_{10}$ species of this report demonstrates that this goal can be realized for a fullerene-based material.

Conclusion

For some years now empty fullerenes, mostly C_{60} and C_{70}, have been readily available.[42] Many applications have been proposed, and after more than a decade of research, their use in electronics[43] and medicine[8−11] now seems imminent. Endohedral metallofullerenes are also expected to contribute to these areas, but their development has been hampered by their low availability.

This contribution reports new methodology whereby highly soluble Gd@C_{60} molecular species have been obtained for the first time by a nonchromatographic procedure. This procedure increases the efficient use of metallofullerene products from the traditional arc synthesis by accessing previously unused M@C_{60}-fraction metallofullerenes. The derivatization procedure solubilizes individual Gd@C_{60} molecules via multiple cycloaddition of bromomalonates, the utility of which has been demonstrated by the production of several hundred milligrams of Gd@C_{60}[C(COOCH$_2$CH$_3$)$_2$]$_{10}$ and Gd@C_{60}[C(COOH)$_2$]$_{10}$.

The potential of Gd@C_{60}[C(COOH)$_2$]$_{10}$ as a new MRI contrast agent has also been evaluated by in vivo MRI biodistribution measurements, relaxometry, and dynamic light scattering. Biodistribution results comparing the M@$C_{2n}(OH)_x$ species with Gd@C_{60}[C(COOH)$_2$]$_{10}$ complement the light-scattering and relaxivity measurements, revealing aggregation for the polyhydroxyl fullerene derivatives but not for the carboxylated fullerene derivative. The emerging pattern is one showing that aggregated polyhydroxyl fullerene derivatives concentrate in the organs of the RES with little or very slow

(40) Qingnuan, L.; Yan, X.; Xiaodong, Z.; Ruili, L.; Qieqie, D.; Xiaoguang, S.; Shaoliang, C.; Wenxin, L. *Nuclear Med. Biol.* **2002**, *29*, 707.
(41) Kato, H.; Yashiro, A.; Mizuno, A.; Nishida, Y.; Kobayashi, K.; Shinohara, H. *Bioorg. Med. Chem. Lett.* **2001**, *11*, 2935.
(42) Krätschmer, W.; Lamb, L. D.; Fostiropoulos, K.; Huffman, D. R. *Nature* **1990**, *347*, 354.
(43) Hinokuma, K.; Ata, M. *Chem. Phys. Lett.* **2001**, *341*, 442.

clearance, while Gd@C_{60}[C(COOH)$_2$]$_{10}$ does not. In fact, this carboxylated metallofullerene derivative is the first fullerene compound proven to exhibit a favorable (non-RES localizing) biodistribution. The development of a nonaggregating and non-RES-targeting fullerene derivative is a significant finding that should contribute to the development of water-soluble fullerene- and metallofullerene-based pharmaceuticals. It now seems reasonable that a variety of fullerene-based materials can be developed for a range of both extra- and intercellular drug delivery.[44] The present report also suggests that metallofullerenes, as derivatized M@C_{60} species, are now more likely to play a role in these developments for medicine and other nanotechnologies as well.

Experimental Section

General. Gd(NO$_3$)$_3$·6H$_2$O (99.9%) was purchased from Strem Chemicals and used as received. All other chemicals were purchased from Sigma-Aldrich and used as received. Solvents were distilled and dried under inert atmosphere according to standard procedures, except for carbon disulfide, which was used as received. Inert atmosphere manipulations were conducted inside a Vacuum Atmospheres glovebox under argon (O_2, H_2O < 5 ppm). Mass spectrometry was performed with two separate instruments having different resolutions; higher-resolution spectra were obtained with a Bruker BiflexTM III MALDI-TOF MS (N_2 laser, $\lambda = 337$ nm), and lower-resolution spectra were obtained with a custom-built laser-desorption combination linear and reflectron time-of-flight mass spectrometer (Nd:YAG laser, $\lambda = 355$ nm). A sulfur matrix deposited from a carbon disulfide solution was used for derivative mass spectra when indicated. Fourier transform infrared spectroscopy was conducted with a Nicolet Magna-IR 550 FTIR spectrometer.

Arc Fullerene Production of Mixed C_{2n}/Gd@C_{2n}. Gd_2O_3 impregnated graphite rods (0.25 in. diameter Poco Graphite, 40% porosity) doped to a level of ca. 1% Gd were produced according to published procedures.[12a] The graphite rods were first evacuated (~1 Torr) and then soaked in a saturated absolute ethanolic solution of Gd(NO$_3$)$_3$·6H$_2$O for 30 min. The solution-saturated rods were air-dried and then heated in a quartz furnace at ca. 850 °C under vacuum for 3 h, converting the metal nitrate to the oxide. Gd-containing fullerene soot was generated by the standard direct current (DC) arc-discharge of Gd_2O_3-impregnated 6 in. graphite rods using a custom-built arc apparatus, operating at 150 Torr of helium. Cathode deposit "back-burning" was employed to maximize the yield of fullerenes and metallofullerenes. "Back-burning" (reverse-polarity arcing) consists of periodically briefly reversing the arc polarity so as to arc the solid deposits of material formed on the cathode (relative to the original polarity). Anaerobic sublimation of the raw arc-produced soot[4,18] onto an isolated, water-cooled coldfinger inside the arc chamber at 750 °C separated the fullerenes (a mixture of soluble and insoluble empty fullerenes and Gd@C_{2n} endohedral metallofullerenes) from the non-fullerene carbon soot. Approximately 2.5 g of sublimed fullerenes (the "sublimate") per 10 rod arc run was obtained.

Separation of the Gd@C_{60} fraction. All soluble fullerenes were then removed from the anaerobically collected sublimate by repeatedly washing with *o*-dichlorobenzene inside the argon-filled glovebox using a continuous-cycling (Soxhlet-style) extractor operating at 40 Torr and 100 °C, until the washings were colorless. Next, the solids were extracted in dichloromethane suspension with a solution of excess tris(*p*-bromophenyl)aminium hexachloroantimonate, which solubilized small amounts of oxidizable Gd@C_{2n} species (e.g., Gd@C_{82} and other Gd@C_{2n}).[20] The solids were separated from the dark-brown filtrate and further treated with aluminum trichloride in *o*-dichlorobenzene to deplete the amount of C_{74}.[4,20] The solids were collected by filtration, rinsed with dichloromethane and hexane, and then dried under vacuum. The resulting material is composed of the Gd@C_{60}-dominated fraction of fullerenes, including chiefly Gd@C_{60} with smaller amounts of Gd@C_{70}, Gd@C_{74}, other higher Gd@C_{2n} and C_{74} (with negligible amounts of C_{60} and C_{70}).

Derivatization of Gd@C_{60}: Synthesis of Gd@C_{60}[C(COOCH$_2$CH$_3$)$_2$]$_{10}$. In a typical synthesis of Gd@C_{60}[C(COOCH$_2$CH$_3$)$_2$]$_{10}$ (conducted in the glovebox), a suspension of Gd@C_{60} (307 mg, 0.350 mmol) and KH (210 mg, 5.25 mmol) (NaH is an acceptable substitute) was prepared in THF (20 mL) with vigorous stirring (15 min). With continued stirring, diethyl bromomalonate (1.255 g, 5.25 mmol) in THF (~1 mL) is added dropwise to the mixture. Vigorous bubbling is immediately observed (evolution of $H_{2(g)}$), and a dark-brown solution color develops within minutes. The mixture was stirred (30 min) after which the dark-brown soluble derivative was separated from excess alkali hydride and small amounts of unreacted fullerene material by filtration (0.45 μm PTFE filter). The product was isolated by THF removal under reduced pressure, rinsed with hexanes, and dried under reduced pressure (yield 331 mg, 41%). FTIR, KBr matrix: C−H aliphatic stretch, 2980, 2927, 2855 cm^{-1}; C═O stretch, 1743 cm^{-1}.

Conversion of Gd@C_{60}[C(COOCH$_2$CH$_3$)$_2$]$_{10}$ to Gd@C_{60}[C(COOH)$_2$]$_{10}$. Conversion of Gd@C_{60}[C(COOCH$_2$CH$_3$)$_2$]$_{10}$ to the water-soluble carboxylate salt Gd@C_{60}[C(COOH)$_2$]$_{10}$ was accomplished by reflux in toluene with NaH followed by a methanol quench, according to the method reported by Lamparth and Hirsch for the conversion of C_{2n}[C(COOCH$_2$CH$_3$)$_2$]$_x$ to C_{2n}[C(COOH)$_2$]$_x$.[28] Lamparth and Hirsch speculate that this transformation takes place via trace nucleophilic OH^- formed by reaction NaH with trace water in the methanol or by hydrogenolysis of the O−Et bonds.[28b] The aqueous-soluble product was converted to the free acid by passage over an acid-form ion-exchange chromatography column (without Gd loss). Next, the solution pH was adjusted to 7.0 with NaOH, and the product was dried under reduced pressure at room temperature. FTIR, KBr matrix: O−H, 3425 cm^{-1} (v br); C═O asymmetric stretch, 1743 cm^{-1}; C═O symmetric stretch, 1146 cm^{-1}.

Relaxivity Measurements. Single-point r_1 relaxivity measurements (expressed by the relationship $(1/T_1)_{obsd} = (1/T_1)_d + r_1$[solute]) in aqueous solution were conducted using an IBM PC/20 MiniSpec Relaxometer operating at 40 °C and a fixed field of 0.47 T (20 MHz). All relaxivity data on Gd metallofullerene compounds calculated the r_1 values in terms of Gd content, which was independently determined by ICP-AES.

Dynamic Light-Scattering Measurements. DLS measurements were performed using a Coulter N4 Plus Dynamic Light Scattering instrument (detection angle 90°) with a lower detection limit of ca. 10 nm in diameter; samples that did not scatter light to a significant degree were judged not to contain particles of sufficient size. DLS measurements in aqueous solution at pH ≈ 7 comparing $C_{60}(OH)_x$, Gd@C_{2n}(OH)$_x$, and Gd@C_{60}[C(COOH)$_2$]$_{10}$ species demonstrated aggregation of the polyhydroxylated compounds (having aggregates in excess of 100 nm diameter), but no such aggregation was observed for the polycarboxylated species.

In Vivo MRI Measurements. To study the MRI contrast and biodistribution behavior of Gd@C_{60}[C(COOH)$_2$]$_{10}$ in vivo, an experiment was performed using a Fischer 344 female rat (Sasco, Wilmington, MA) weighing 200−220 g and housed at the Department of Veterinary Medicine and Surgery, University of Texas, M. D. Anderson Cancer Center (Houston, TX) with all procedures conforming to institutional guidelines for animal welfare. The rat was injected via the tail vein with 1 mL of a 3 mM solution of Gd@C_{60}[C(COOH)$_2$]$_{10}$ in saline at pH = 7.4. The dosage was approximately 35 mg/kg, which was well tolerated by the animal. Images were acquired on a 1.5 T GE LX EchoSpeed scanner (GE Medical Systems, Milwaukee, WI) using a custom spiral surface coil. The animal was scanned in the prone position

(44) Wharton, T.; Kini, V. U.; Mortis, R. A.; Wilson, L. J. *Tetrahedron Lett.* **2001**, *42*, 5159.

in the MRI experiment. Prior to contrast agent administration, coronal flow-compensated T_1-weighted fast spin−echo images were acquired from 18 2-mm contiguous sections (echo time of 15 ms, repetition time of 400 ms, echo train length of 2, field-of-view of 12 cm × 12 cm, 256 × 192 matrix, four averages). Immediately before, during, and after contrast agent administration, a dynamic fast spin−echo sequence was used to acquire T_1-weighted images from 5 2-mm sections (with 2-mm gaps) with a temporal resolution of 11 s (echo time of 14 ms, repetition time of 400 ms, echo train length of 4, field-of-view of 12 cm × 9 cm, 256 × 128 matrix, one average). The total duration of the dynamic scanning sequence was 5 min. Following the dynamic acquisition, fast spin−echo T_1-weighted images were acquired from the 18 2-mm contiguous sections (using the parameters listed above) at 10-, 20-, 30-, and 45-min post-contrast agent infusion.

Acknowledgment. We thank the NIH for support (SBIR Grant 5-R44-CA66383 and Grant 1-R01-EB000703). L.J.W. thanks the Robert A. Welch Foundation (Grant C-0627) for additional support.

Supporting Information Available: Mass spectra of Gd@C_{2n} containing arc-produced soot and sublimate (PDF). This material is available free of charge via the Internet at http://pubs.acs.org.

JA0340984